

<sup>5</sup> Fisher, R. R. and Lown, R. C., "Test results, developments, and structural applications of expandable structures for advanced marine vehicles," Goodyear Aerospace Corp. Rept. GER 11854 (December 1964).

<sup>6</sup> Gonsalves, J., "Design study for establishing an open-ocean tilt-float configuration helicopter," Vertol Div., Boeing Rept. R-452 (January 1966).

<sup>7</sup> Fritzsche, H. J., "A feasibility study for applying the tilt float principle to the Curtiss Wright X-19 aircraft," Curtiss Wright Corp., VTOL Systems Div. Rept. 014-537 (March 1965).

<sup>8</sup> Allen, E. M. and Dyke, R. W., "Investigation of overwater aspects of VTOL aircraft at high disc loading," Curtiss Wright Corp., VTOL Systems Div. Rept. 012-26 (December 1964).

<sup>9</sup> Brown, P., "The effect of configuration on the drag of oscillating damping plates," Davidson Lab., Stevens Institute of Technology, Rept. 1021 (May 1964).

<sup>10</sup> Marsh, K. R., "Feasibility study, XC-142A modified for open ocean operation," LTV Vought Aeronautics Div., Rept. 2-55400/4R-963 (February 1965).

<sup>11</sup> Dewey, D. B., Jr. and Fisher, R. R., "Inflatable float design study," General Dynamics/Convair Final Rept. 65-193 (September 1965).

<sup>12</sup> Breslin, J. P., Savitsky, D., Tsakonas, S., "Deterministic evaluation of motions of marine craft in irregular seas," Davidson Lab., Stevens Institute of Technology, TN 723 (1964).

<sup>13</sup> Barr, R. A. and Martin, M., "Motions of tilt float vehicles in waves," Hydronautics Inc. Rept. TR 237-1 (October 1963).

NOV.-DEC. 1966

J. AIRCRAFT

VOL. 3, NO. 6

## Propulsion System Development for V/STOL Transports

J. T. KUTNEY\*

*General Electric Company, Cincinnati, Ohio*

The evolution and technology development of the high bypass ratio tip turbine lift fan and lift/cruise fan propulsion systems are presented. The characteristics of the high bypass propulsion system are reviewed and compared to other subsonic propulsion concepts. Fundamental aerothermodynamic aspects of the system are examined, including internal and external aerodynamics. Significant results from extensive mechanical and aerodynamic scale model and full-scale investigations are presented. Suggested aircraft applications in light and medium V/STOL transports based on this technology are presented.

### Nomenclature

|                         |  |
|-------------------------|--|
| $TJ$                    | = turbojet   |
| $TF$                    | = low bypass ratio turbofan engine   |
| $L/CF$                  | = high bypass ratio tip turbine lift/cruise fan                              |
| $F_G$                   | = gross thrust   |
| $F_N$                   | = net thrust   |
| $C_{T-D}$               | = installed thrust coefficient = (measured thrust minus drag)/(ideal thrust) |
| $P_{TN}$                | = nozzle total pressure  |
| $P$                     | = ambient pressure   |
| $C_{DT}$                | = total nacelle drag coefficient = $D/q_0 A$                                 |
| $C_{DBT}$               | = afterbody boattail drag coefficient = $D/q_0 A$                            |
| $C_{DFB}$               | = forebody pressure drag coefficient = $D/q_0 A$                             |
| $C_{DF}$                | = friction drag coefficient = $D/q_0 A$                                      |
| $T_D$                   | = drive flow temperature   |
| $T_0$                   | = ambient temperature  |
| $N/\theta^{1/2}$        | = rotor corrected speed  |
| $W/\theta^{1/2}/\delta$ | = drive corrected flow   |
| $P_{Tj\delta}$          | = drive corrected pressure   |
| $BPR$                   | = bypass ratio   |

### Introduction

STUDIES conducted by the General Electric Company in 1957 under sponsorship of the Transportation Research Command of the U. S. Army (TRECOT) indicated that one of the systems that showed considerable promise was a con-

vertible system that used the jet engine for cruise flight and a lift fan driven by turbine buckets mounted at the tips of the fan rotor for takeoff and landing. These two components are coupled pneumatically through a diverter valve that enables the same gas generator to be used for both lift and cruise.

The initial phases of the development of this propulsion system have been completed and over 600 hr of full-scale static and wind-tunnel operation have been demonstrated successfully, culminating in the XV5A research aircraft application.

The initial lift fan concept was designed specifically for wing mounting or adapted to fuselage mounting but always with turbojet operation for the cruise mode. The aircraft were surveillance-type cruising at  $M = 0.8$ . Subsonic transport aircraft cruising at  $M = 0.7$  to  $M = 0.8$  will not be powered by turbojet engines, since fans offer such great economy. With this basic philosophy in mind, General Electric has conducted many studies to combine the obvious advantages of the lift fan into a high bypass ratio system. Thus, was born the lift/cruise fan.

Some of the significant aspects of a development program including system studies, full-scale, and scale-model technology designed to demonstrate the system performance for the lift/cruise fan are given in this paper.

### Discussion

The original lift fan system was made as 'thin' as possible so as to fit between the spars of a 10% thick wing. Initial testing at NASA Ames included both fan in fuselage and fan in wing configurations as shown in Fig. 1. Both the fan in wing and fan in fuselage installations demonstrated predictable performance, the lift being approximately 2.8 times the J85 turbojet thrust. The fan tip diameter of 62.5 in. for the fan

Presented as Preprint 64-606 at the AIAA Transport Design & Operations Meeting, Seattle, Wash., August 10-12, 1964; revision received August 11, 1965. The author wishes to thank the Transportation Research Command of the U. S. Army for permission to discuss the results of the scale model nacelle testing; Fluidyne for their cooperation; Tech Development of Dayton, Ohio, the manufacturer of the scale model cruise fan; and the members of V/STOL Operation of General Electric whose work made this paper possible.

\* Manager, GE1/6 Installation Aerodynamics, Advanced Engine and Technology Department. Member AIAA.

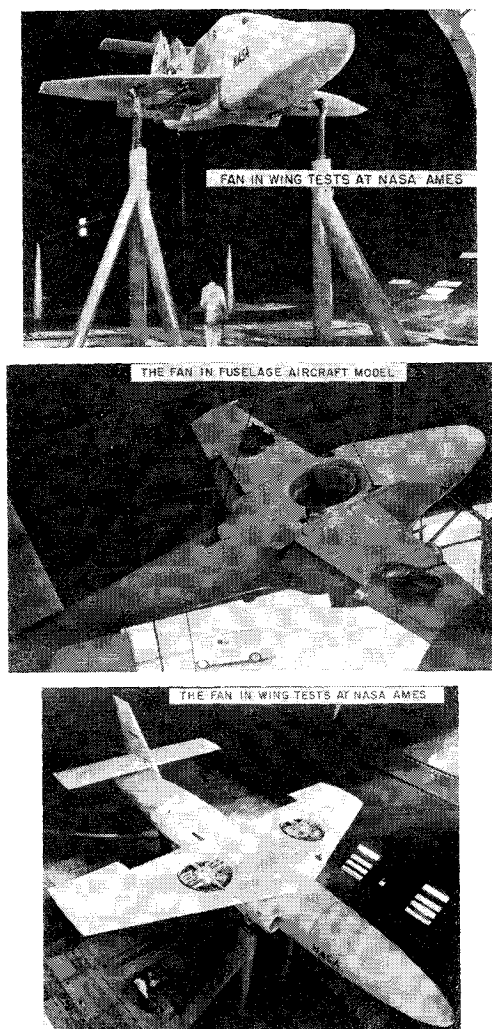


Fig. 1 Full-scale lift fan testing.

rotor had been chosen based on tradeoff studies of weight, diameter, lift, and lift-to-weight ratio. In order to minimize installed dimension between the wing spars, it was decided to make the turbine a partial admission design so space would not be required for ducting the propulsion gas to fill the outer half of the turbine.

This combination of gas generator, diverter valve, and lift fan can be used logically for cruise propulsion by turning the lift fan 90° as shown in Fig. 2. For illustration purposes, the partial admission turbine is not change in this figure, although this is a very significant difference between the lift fan and the lift/cruise fan. The lift/cruise fan system is basically an aft fan arrangement where the fan is not coaxial with the gas generator and all of the exhaust energy of the gas generator is extracted to drive the tip turbine fan system.

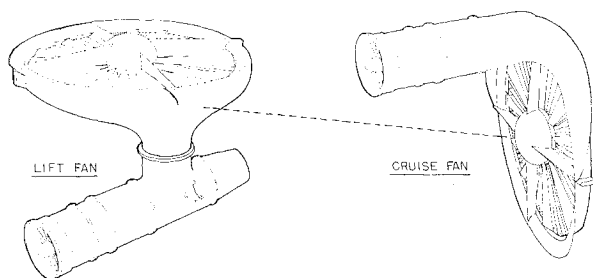


Fig. 2 Evolution of a tip turbine cruise fan from a tip turbine lift fan.

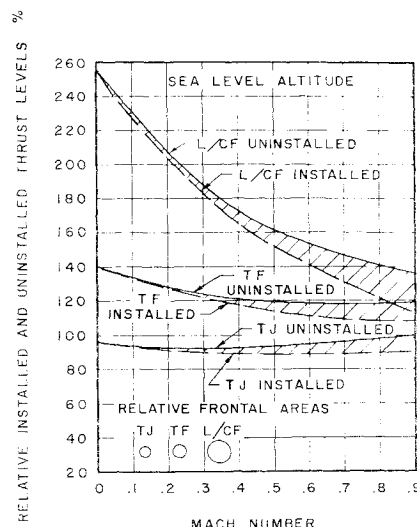


Fig. 3 Turbojet, turbofan, and lift/cruise fan thrust vs Mach number characteristics.

### Thermodynamic Analysis

Thermodynamic studies are presented in Figs. 3 and 4 to show the basic differences between the turbojet (*TJ*), low bypass turbofan (*TF*), and the lift/cruise fan (*L/CF*) cycles. In these analyses, the systems all utilize the same gas generator as a basic power unit. In each case, the gas generator is assumed to be operating at the same power setting, and bypass ratio changes are assumed to be achieved with the over-all gas generator compression ratio being held constant. The gas generator cycle used in these studies represents modern day technologies of 13:1 compression ratio and 2000° turbine inlet temperature.

These data show a clear and significant advantage for the lift/cruise fan system compared to the turbojet and the low bypass turbofan, both on an uninstalled and on an installed basis. These data also indicate the high subsonic speed potential of the lift/cruise fan system together with the thrust augmentation at takeoff conditions.

System weight studies provide another performance advantage for the lift fan system as shown in Fig. 5. Since V/STOL transports are expected to require hovering times greater

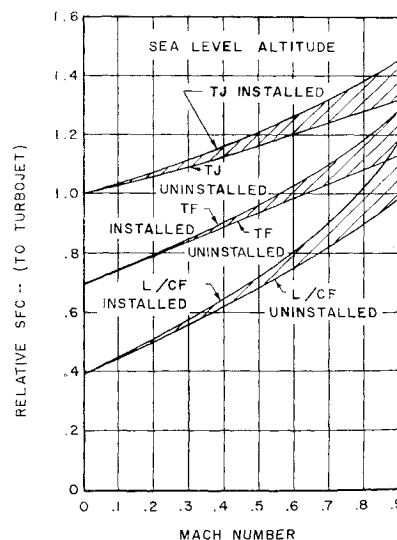


Fig. 4 Turbojet, turbofan, and lift/cruise fan sfc vs Mach number characteristics.

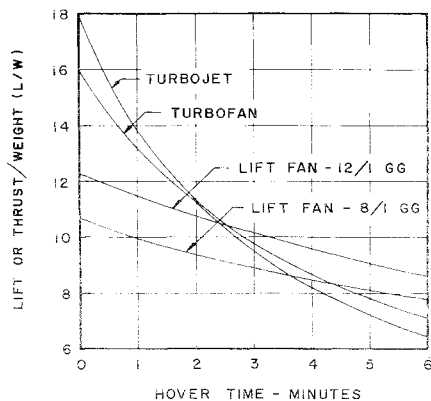


Fig. 5 Lift/weight (engine plus fuel) vs hover time.

than 6 min, the high bypass fan system is shown to have a significant lift-to-weight ratio advantage.

These weight studies also have demonstrated that coupling the lift/cruise fan system to the gas generator results in an increase in the basic gas generator and fan thrust to weight ratio at sea level conditions relative to a turbojet, as shown in Fig. 6. At a bypass ratio of 10, the  $T/W$  ratio is 25%

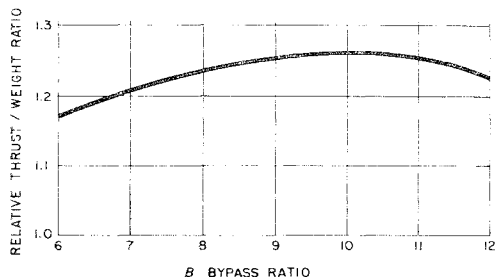


Fig. 6 Uninstalled thrust/weight ratio of tip turbine cruise fans at sea level (relative to turbojet).

greater than for a turbojet. These data do not include nacelle cowlings and therefore are uninstalled, but include all the components required for test cell running.

### Lift Cruise Fan Geometry

The evolution of the lift/cruise fan from the lift fan retained the basic tip turbine concept; however, there is a considerable change in design philosophy as dictated by the need for high speed forward flight requirements. In Fig. 7, the envelope of the lift/cruise fan is compared to typical turbofan configurations. The concentric front fan and concentric aft fan configurations are the familiar types found in today's aircraft.

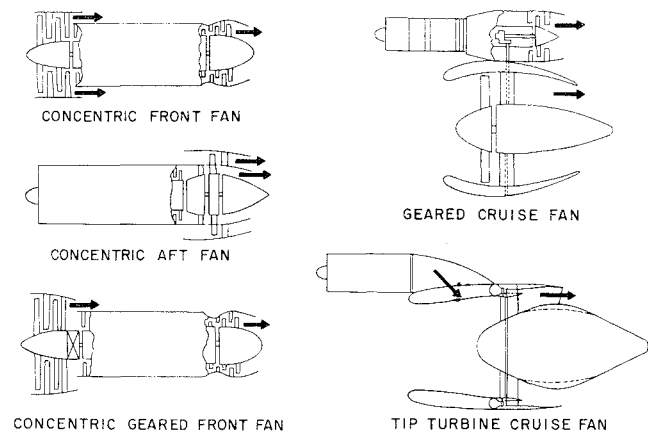


Fig. 7 Typical turbofan configurations.

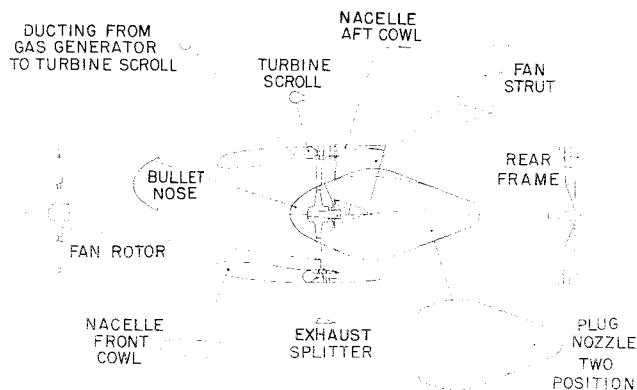
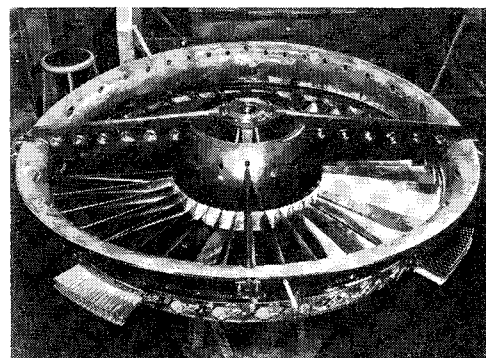


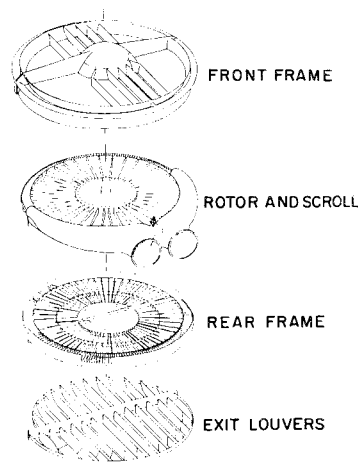
Fig. 8 Mechanical parts breakdown: tip turbine cruise fan.

These configurations have bypass ratios from 1 to 2.0. As the bypass ratio is increased to higher values in the 10 to 15 range, it may become desirable to use a gearbox in the concentric fan to maintain the desired ratio of fan to turbine speed. For bypass ratios in the 6 to 15 range, and unique remote fan arrangements, the geared parallel fan and tip-turbine cruise fan can be considered.

The mechanical parts breakdown for the tip-turbine lift/cruise fan system is shown in Fig. 8. Unlike the lift fan discussed previously, the lift/cruise fan incorporates a full admission arrangement with the ducts from the gas generator exhaust enveloped in a high speed nacelle cowl shape. The flow from the turbine covers the outer periphery only with fan flow exhausting through the center portion of the nacelle. This feature has been used to incorporate a unique two position nozzle for high-speed operation. This two-position nozzle is the only control in the lift/cruise fan other than the normal gas generator controls.



a) X353-3 lift fan hardware



b) Exploded view of lift fan

Fig. 9 X353-3 lift fan hardware exploded view of lift fan.

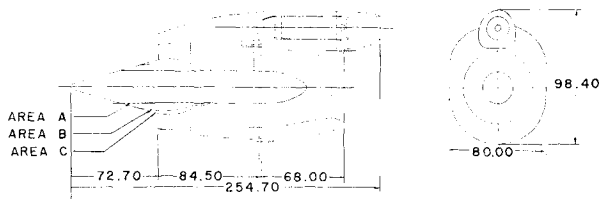


Fig. 10 X353-5 cruise fan nacelle.

### Full-Scale Lift/Cruise Fan Demonstration

In order to provide early test information on full-scale hardware, the lift fan system was adapted to a cruise fan configuration and tested in the NASA Ames 40- X 80-ft wind tunnel. The fan used in the test program was the same lift fan hardware used in the previous extensive lift fan investigations. The only modifications to the basic lift fan hardware for this test were the removal of the inlet and exit louver hardware. The basic lift fan hardware is shown on Fig. 9.

A YJ85-5 engine was used to power the fan. A close coupled engine-fan combination as shown in Fig. 10 was used for the test configuration. In this arrangement, the exhaust gases from the gas generator are collected and turned into the partial admission tip turbine by a specially designed scroll system. The fan internal flow passage was symmetrical about the fan axis; however, the partial admission arc of the basic lift fan influenced the design of the nacelle to be non-circular as shown in Fig. 10. The inlet characteristics were designed to have high subsonic drag divergent Mach number characteristics. The afterbody was a circular arc design with a terminal boattail angle of  $10^\circ$  at the  $180^\circ$  meridian varying to  $23^\circ$  at the  $0^\circ$  meridian.

The cruise fan was provided with a variable exhaust area system designed to achieve optimum area performance from static through maximum simulated speed conditions. These nozzle area variations were obtained by changes in plug nozzle hardware.

The model was supported by two 8-in.-diam trunnion supports, which in turn were connected to the pitching mechanism giving  $-4^\circ$  to  $90^\circ$  duct angle-of-attack variation. The test model was instrumented extensively with internal and external pressure instrumentation. A pictorial description of this bypass ratio of 12 lift/cruise fan system is given in Figs. 11 and 12.

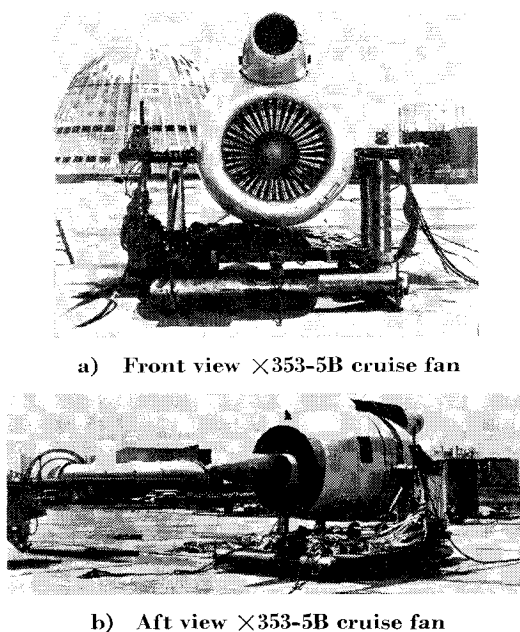
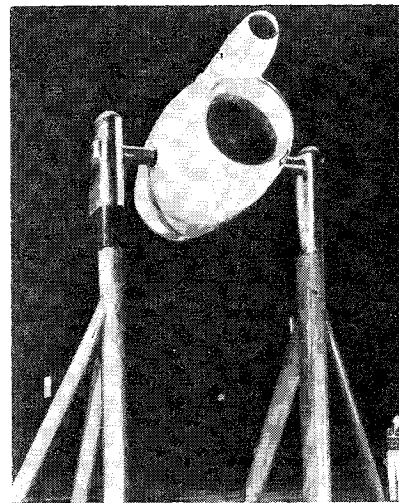
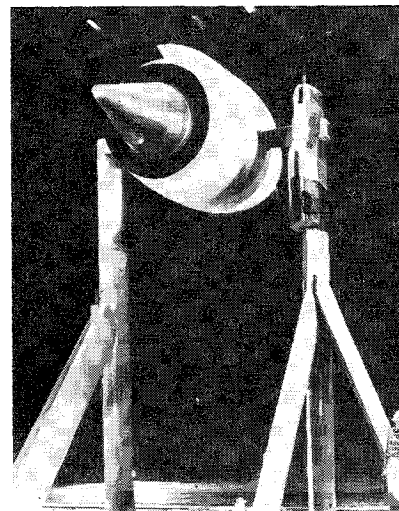


Fig. 11 Front and aft view X353-5B cruise fan.



a) Front view



b) Aft view

Fig. 12 X353-5B cruise fan test model, NASA Ames Research Center: front and aft view.

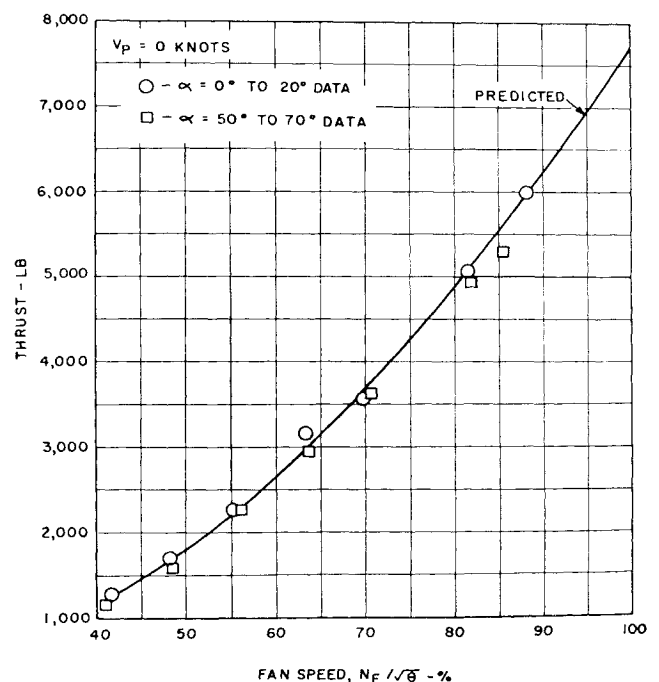


Fig. 13 Ames cruise fan test actual vs predicted thrust.

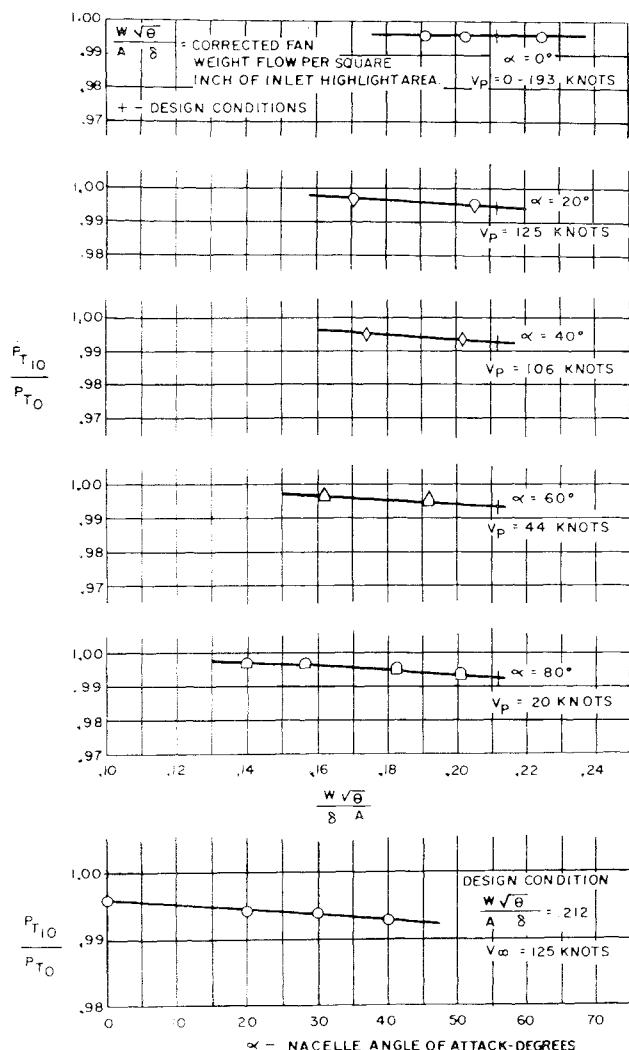


Fig. 14 Ames cruise fan test inlet recovery data at angle of attack.

The test objectives were to obtain over-all system performance, verify design assumptions and calculations, and to establish over-all system feasibility. A total of 320 data

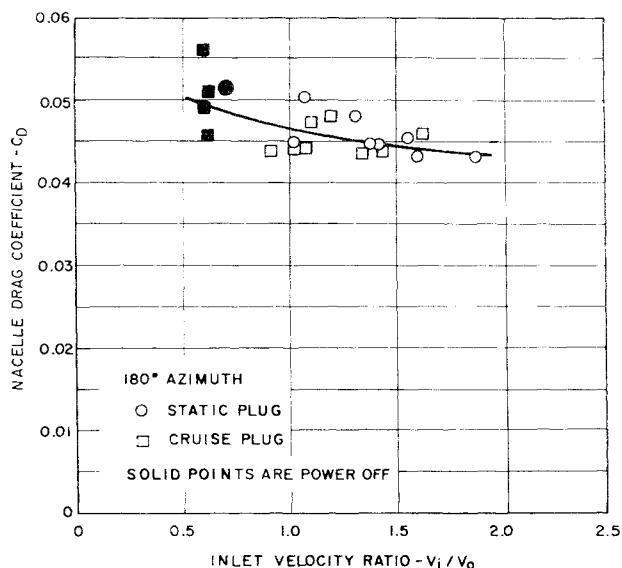


Fig. 15 X353-5 cruise fan, Ames test nacelle drag coefficient (total pressure integration vs inlet velocity ratio).

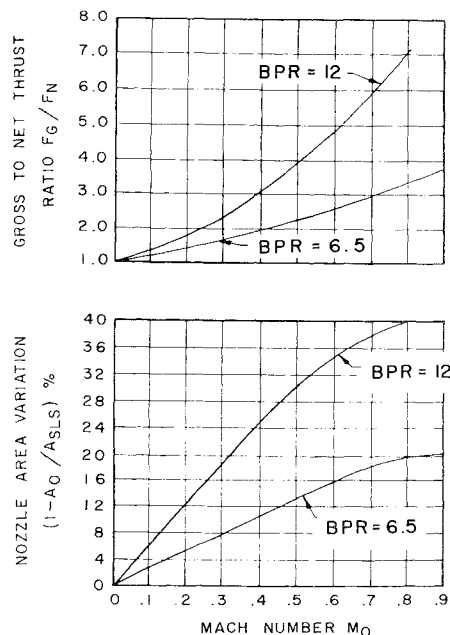


Fig. 16 Lift/cruise fan exhaust nozzle parameters vs Mach number.

points were taken, of which 290 were fan powered. The following range of variables were investigated: 1) tunnel velocity, 0 to 180 knots; 2) nacelle angle of attack,  $-4^\circ$  to  $80^\circ$ ; 3) fan speed, 0 to 100%; 4) nozzle area, 63, 87, 100% open area.

The significant test results are included in Figs. 13-15. The measured thrust levels demonstrate that the performance assumptions used in the calculations were correct and thus verify the capability of predicting internal system performance.

The nacelle inlet was designed to achieve good inlet recovery at all angles of attack without the need for a variable inlet and the attendant hardware complexity. The test data show recoveries over 0.995 at low angles of attack and over 0.990 at all angles of attack tested. The test data showed no lip separation below  $60^\circ$  angle of attack. At  $60^\circ$  and above, lip separation could be induced by a combination of high tunnel speed and low fan speed. A hysteresis phenomenon is present, which requires a large decrease in flight velocity and/or increase in fan rpm to reattach the flow after separation.

The nacelle external drag was obtained by several methods, including meridional static pressure integration and total pressure measurements obtained by rakes located at the nozzle

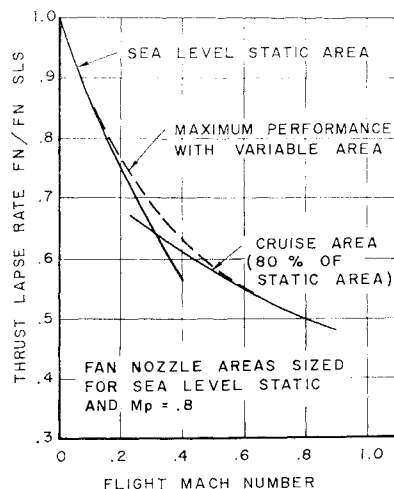
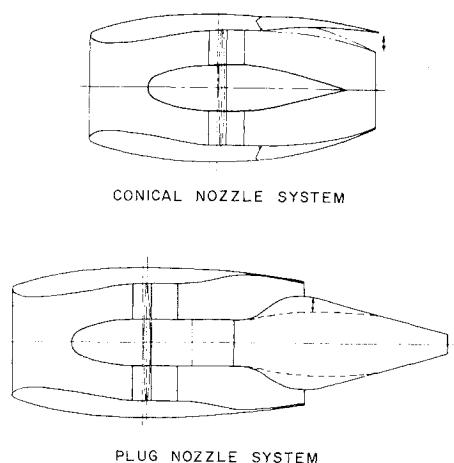


Fig. 17 Thrust lapse rate with two position nozzle.



**Fig. 18 Comparison of conical and plug nozzle cruise fan systems.**

exit plane. The variation of drag coefficient at the 180 degree azimuth is presented in Fig. 15 as a function of inlet velocity ratio and nozzle geometry. This position was chosen because it represents an area of symmetry and was not affected by support-strut effects and is most representative of a true lift/cruise fan nacelle.

This external drag coefficient includes the effects of form and friction drag over the entire nacelle, but does not consider the nozzle plug as part of the control volume. Since the

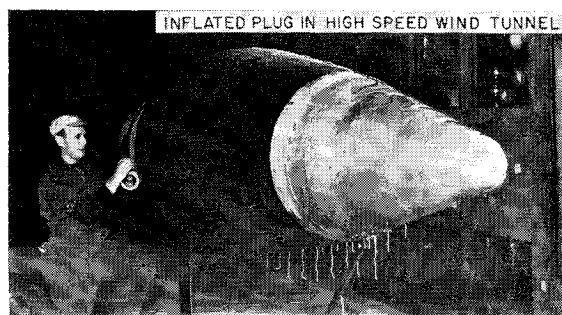
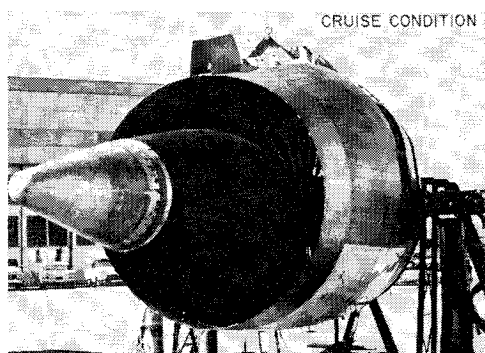
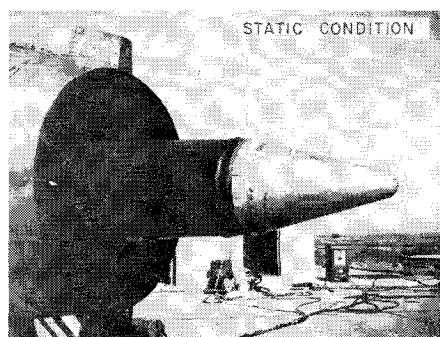


**Fig. 19 Full-scale two-position inflatable plug nozzle.**

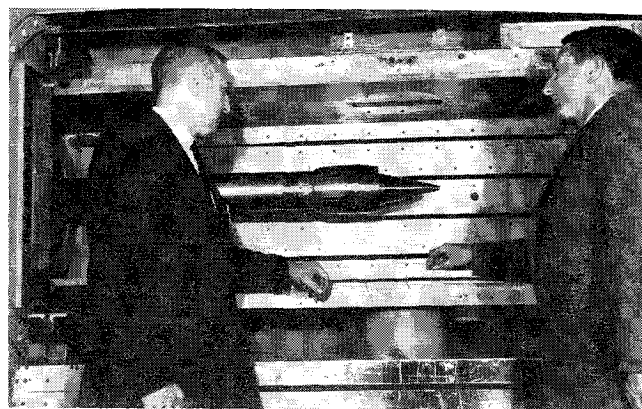


**Fig. 20 Plug nozzle configuration installed in transonic wind tunnel.**

external flow results in a change in plug forces, this would be included logically in the drag coefficient and lower the drag coefficient in Fig. 15.

### Exhaust Nozzle Methodology

Analysis indicates that the exhaust nozzle performance has a significant effect on total system performance and is a criterion in establishing fan bypass ratio. Since nozzle performance is defined in gross thrust levels, the ratio of gross to net thrust determines the sensitivity of nozzle performance to the net propulsive effort of the system.

This is demonstrated in Fig. 16 where the bypass ratio 12 system has a 7 to 1 multiplying effect at  $M = 0.8$ , and the bypass ratio 6.5 system has a 3.5 multiplying effect at  $M = 0.8$ . The area variation required for optimum fan performance also is influenced severely by bypass ratio levels with the higher bypass system requiring 40% area variation at  $M = 0.8$  and the lower bypass fan only half as much. A typical low bypass turbofan (CJ805-23) requires no area variation and has a gross to net thrust ratio of slightly over 2.0 at  $M = 0.8$ .

Thermodynamic analysis indicates that a two position nozzle may be satisfactory to cover the entire range from  $M = 0$  to  $M = 0.8$ . Figure 17 shows the thrust lapse rate for a two-position concept and also for a continuously variable nozzle system. It is seen that only at  $M = 0.3$  is there a significant thrust loss and this is in the order of 7%. The exact flight spectrum where this loss occurs can be adjusted by selective nozzle area selection.

The types of nozzle arrangements which appear suitable for the lift/cruise fan are the conical and plug types as shown in Fig. 18. The plug type appears to have advantages of performance, simplicity, and weight and is considered preferable.

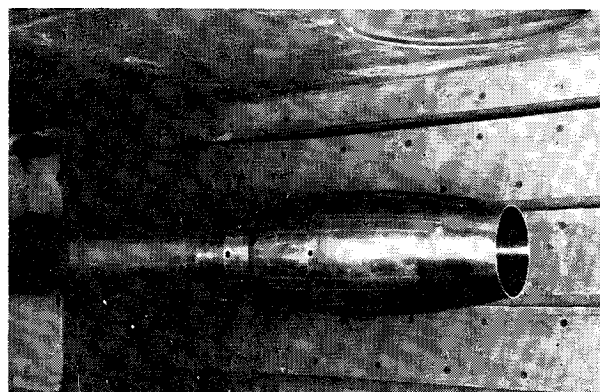


**Fig. 21 Close view convergent nozzle configuration.**

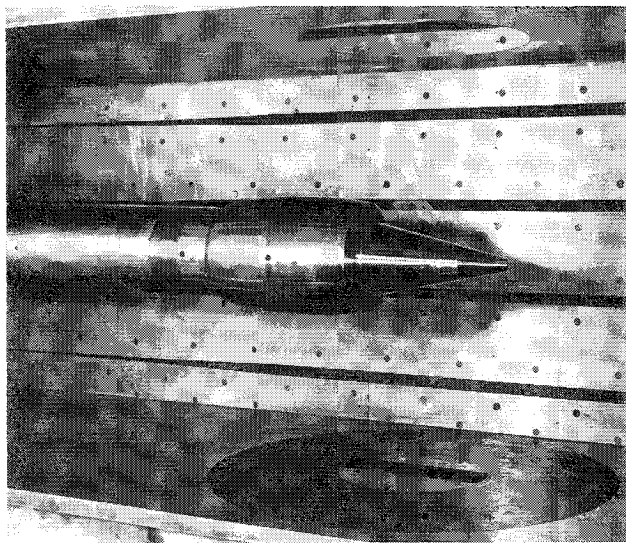


Fig. 22 Side view of plug nozzle configuration.

Full-scale development activity on the plug type has included the inflatable rubber centerbody shown in Fig. 19. The rubber boot is shown in the deflated or static condition and in the inflated or cruise mode. The boot has been tested up to Mach 0.9 in the high-speed wind tunnel and no serious variations in shape were present.

Scale-Model Nacelle Technology

The full-scale lift/cruise fan testing could not provide the complete experimental variation of parameters because of fan pressure ratio limitations and wind-tunnel speed limitations. Therefore, a scale-model nacelle and nozzle research program was conducted under the sponsorship of TRECOM. This program was designed to obtain design data for high bypass ratio lift/cruise fan exhaust systems.

The resultant data are applicable to all types of cruise fans, tip turbine, or geared systems. The testing was conducted in a 22- X 22-in. slotted wall wind tunnel at FluiDyne Engineering Corporation, Minneapolis, Minn. This tunnel is an induction-type facility whereby atmospheric air is drawn through the test section using steam ejectors to reduce the downstream pressure. Models and the balance system are supported in the test section by a 5-in.-diam tube that contains the main air supply.

The facility is equipped with an internal force balance that measures the combined effect of nozzle internal and nacelle external flows. Both plug nozzles and conical nozzles

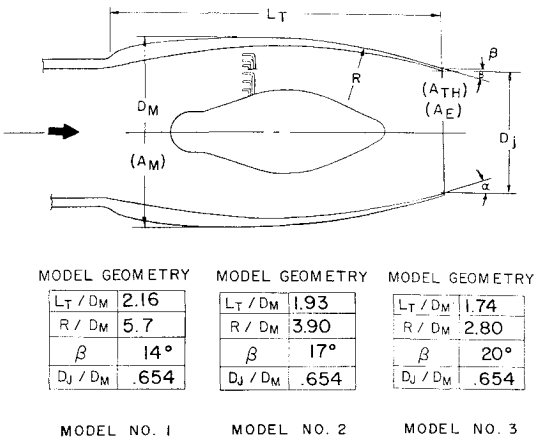


Fig. 23 Conical nozzle model details.

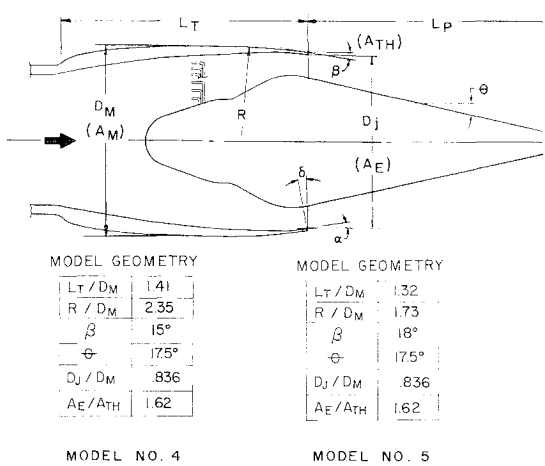


Fig. 24 Plug nozzle model details.

were evaluated in this research program. Figures 20-22 illustrate the model geometry as installed in the wind tunnel.

Selected configurations from this program are presented in this paper. Configurations 1, 2, and 3 as shown in Fig. 23 are conical nozzle installations, whereas Fig. 24 defines two of the plug nozzle configurations, models 4 and 5.

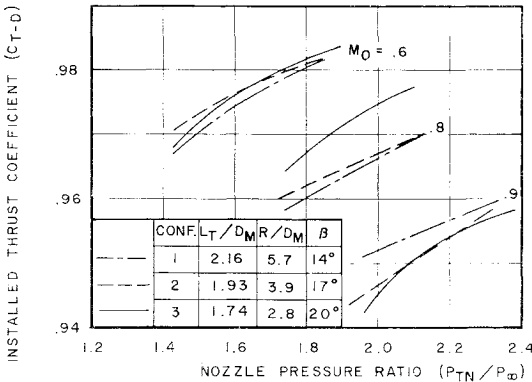


Fig. 25 Performance comparison of conical exhaust systems with external flow.

The three conical nozzle systems differed only in boattail geometry. Figure 25 indicates that up to  $M = 0.8$  performance increases slightly with decreased length and boattails up to 20° are not too great, but at  $M = 0.9$  the lowest boattail angle had the best installed performance. This shows that pressure or from drag predominates at  $M = 0.9$ , but that friction drag is more critical at lower Mach numbers. Radius ratios of 2.8 are acceptable, therefore, for lift/cruise systems for  $M = 0.8$  and lower.

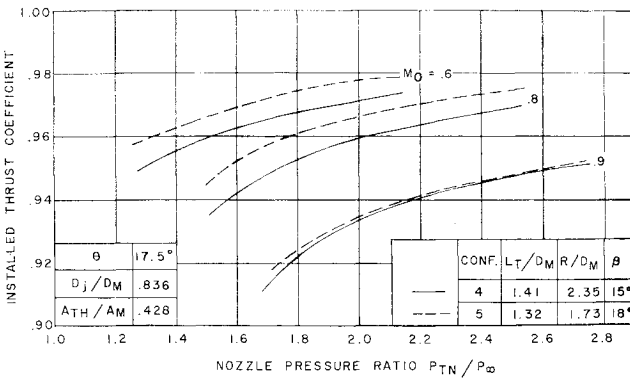


Fig. 26 Comparison of plug nozzle performance with external flow.



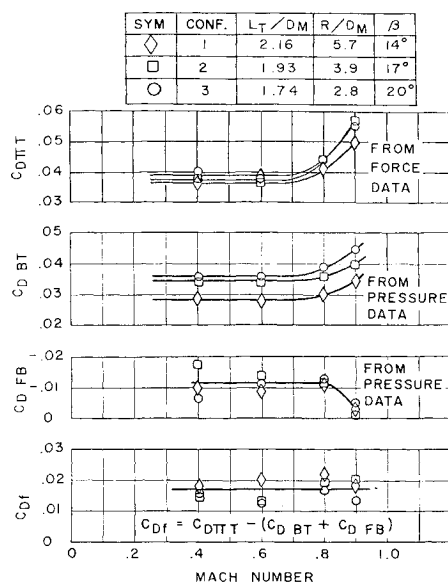


Fig. 27 Installed breakdown of models 1, 2, and 3.

The plug nozzle geometries displayed the same type of emphasis on skin friction as did the conical nozzle systems. Configuration 5 as shown in Fig. 26 with a steeper boattail angle, lower shroud length, and lower radius ratio performed better at all Mach numbers. These data indicate that both types of nozzle system show very good installed performance.

A breakdown of installed performance or friction and boat-tail drags is presented in Fig. 27 for the conical nozzle systems. This analysis shows the compensating effects of boat-tail drag and friction resulting in approximately the same drag coefficient for models 1, 2, and 3.

The nacelle boat-tail pressure drag is influenced uniquely by the local surface Mach number. The nacelle boat-tail curvature of the models tested was analyzed, and the critical Mach number was determined as a function of the boat-tail radius ratio as shown in Fig. 28. According to this analysis, the radius ratio can be designed at 1.75 for cruise Mach numbers of 0.8 or less. The onset of local sonic flow is not in itself an indication of separation, as none of the models tested showed any boat-tail flow separation.

### Scale-Model Tip Turbine Cruise Fan

The test program was designed to investigate nozzle and nacelle effects, for cruise fan technology could not include inlet mass flow ratio effects on nacelle drags and nozzle performance. To extend the technology into this area, specially designed scale-model cruise fans have been developed as shown in Fig. 29. This fan is driven by tip turbines mounted at the fan rotor and driven by cold high-pressure air with the quality as shown in Fig. 30. The fans were designed to have a 1.20 pressure ratio at 23,000 rpm. Figure 31 presents the area weighted pressure ratio, whereas Fig. 32 shows the pres-

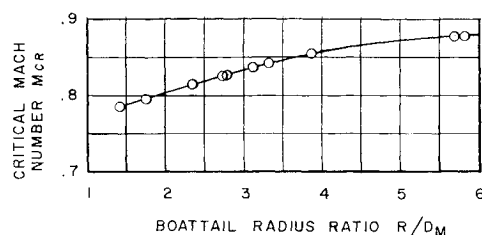
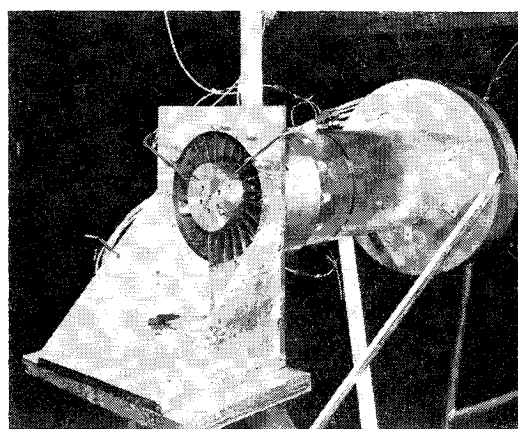
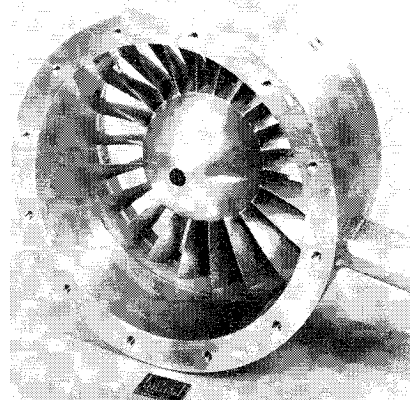


Fig. 28 Nacelle boat-tail curvature vs critical Mach number.



a) Front view



b) Calibration installation

Fig. 29 Scale-model tip turbine cruise fan.

sure profiles at various rotor speeds. It is of particular interest to note that the pressure element located at 2.02 in. is in the tip turbine annulus and shows that the turbine efflux is not significantly different from the main fan flow. This fan system has many potential aerodynamic uses in V/STOL technology, including interference drag investigations.

### Aircraft Applications

These test data and the previously successful lift fan test programs have confirmed that this type of propulsion system can be combined in an attractive V/STOL transport configuration. A suggested arrangement is illustrated in Fig. 33.

This transport configuration combines the proven fan-in wing lift fan technology with the technology from the programs discussed in this paper in a high speed configuration applicable to 4- to 10-ton payload sizes. The areas for further investigation include the folding fan philosophy, both mechanical and aerodynamic interaction phenomena as well as the mechanical rotation feature of the lift/cruise fans. Studies have been conducted of ducting designs that allow thin pylons to be used for the nacelle and fuselage junction.

In this transport configuration, all fan systems are interconnected such that the loss of any single gas generator results in an evenly distributed 18% lift loss in a 4 engine, 4-ton transport and an evenly distributed 9% lift loss in an 8 engine, 10-ton assault transport. The interconnecting ducting further provides the ability to allow more flow and hence more lift to any discreet location for aircraft control purposes by fan overspeed.

### Conclusion

The tip turbine lift fan system combined with the lift/cruise fan system offers the potential of having a V/STOL



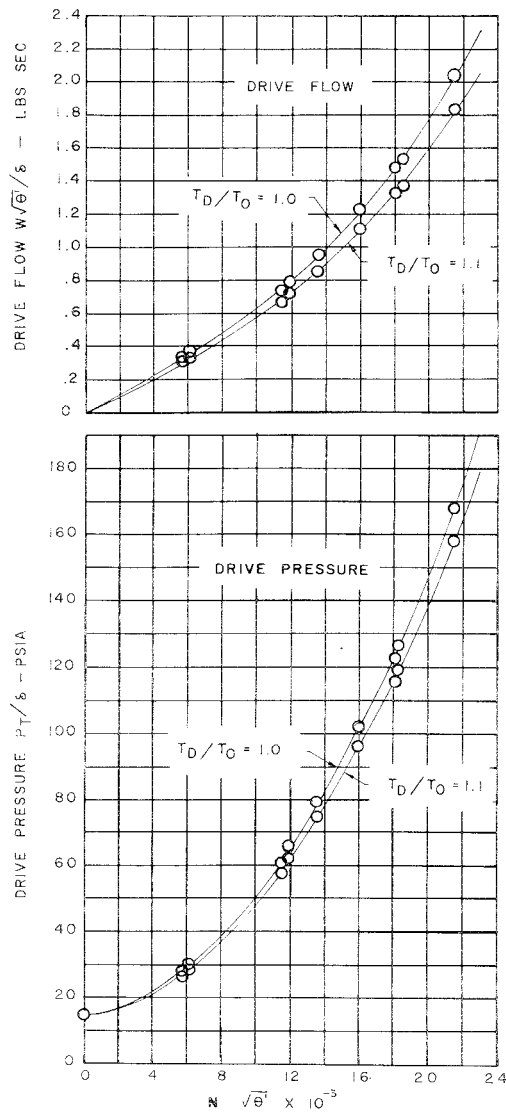


Fig. 30 Fan drive parameters vs rotor corrected speed.

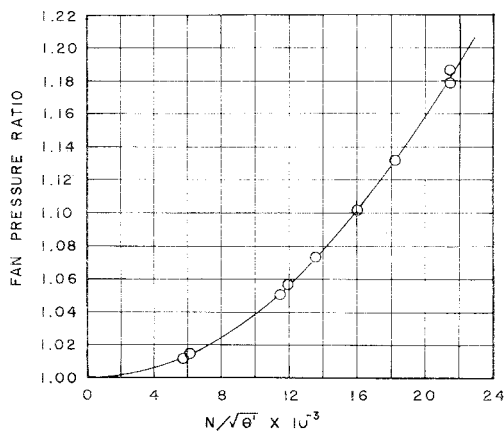


Fig. 31 Fan pressure ratio vs corrected speed.

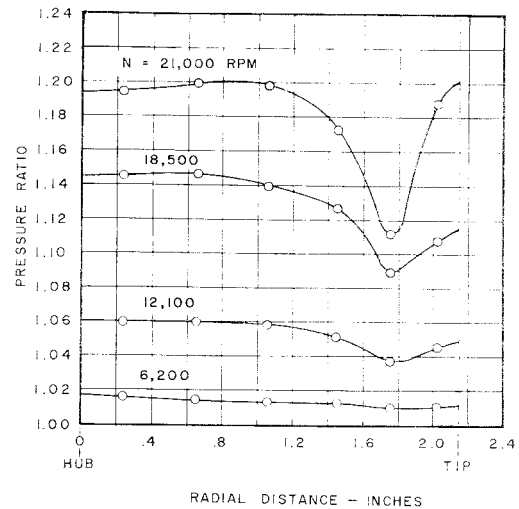
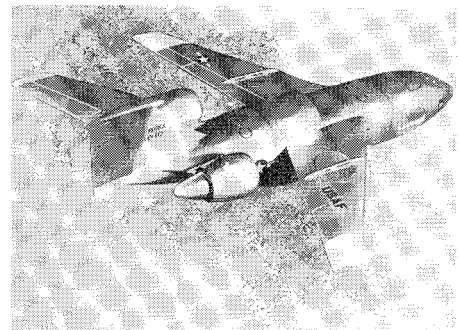
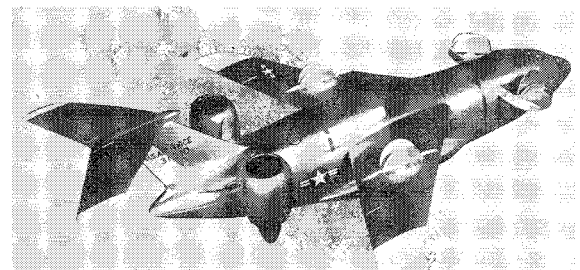


Fig. 32 Pressure profile vs radial distance.



a) Cruise mode



b) VTOL mode

Fig. 33 V/STOL transport configuration with tip turbine lift fans and lift/cruise fans.

transport with a single type of gas generator, while achieving the desirable thrust match and low SFC characteristics of fans for lift and landing and for high subsonic cruise. Considerable technology programs have been conducted which have provided design verification for the propulsion system. All mechanical systems and performance assumptions have been demonstrated successfully.

### Reference

<sup>1</sup> Guilianetti, D. J., Biggers, J. C., and Corsiglia, V. J., "Wind tunnel test of a full-scale, 1.1 pressure ratio, ducted lift-cruise fan," NASA TN D-2498 (1964).